



## Effect of Magnetic Material Nonlinearities on the Acoustic Behavior of 4-phase SRMs

Haifa Mechmeche, Michel Hecquet, Abdelmounaïm Tounzi, Frederic Gillon,  
Guillaume Fritz

### ► To cite this version:

Haifa Mechmeche, Michel Hecquet, Abdelmounaïm Tounzi, Frederic Gillon, Guillaume Fritz. Effect of Magnetic Material Nonlinearities on the Acoustic Behavior of 4-phase SRMs. ICEM, International Conference Of Electrical Machines, 2014, Berlin, Germany. hal-01730153

HAL Id: hal-01730153

<https://hal.science/hal-01730153v1>

Submitted on 13 Mar 2018

**HAL** is a multi-disciplinary open access archive for the deposit and dissemination of scientific research documents, whether they are published or not. The documents may come from teaching and research institutions in France or abroad, or from public or private research centers.

L'archive ouverte pluridisciplinaire **HAL**, est destinée au dépôt et à la diffusion de documents scientifiques de niveau recherche, publiés ou non, émanant des établissements d'enseignement et de recherche français ou étrangers, des laboratoires publics ou privés.

# Effect of Magnetic Material Nonlinearities on the Acoustic Behavior of 4-phase SRMs

H. Mechmeche<sup>1,2</sup>, M. Hecquet<sup>1</sup>, A. Tounzi<sup>1</sup>, F. Gillon<sup>1</sup>, and G. Fritz<sup>2</sup>

**Abstract** – The aim of this paper is to study the saturation effect on the electromagnetic and acoustic behavior of Switched Reluctance Machines (SRMs). Two 4-phase SRMs (8/6 and 16/12) are analyzed through numerical models under the hypothesis of linear and nonlinear magnetic material characteristics. The harmonic content of the radial Maxwell pressure and the radiated acoustic power are compared in both qualitative and quantitative terms. The results show that, in opposite case to induction and synchronous machines, the saturation phenomenon does not increase the harmonic content of the electromagnetic fields of SRMs and even leads to reduce their radiated acoustic power.

**Index Terms**—Saturation, Nonlinearities, Switched Reluctance Motors, Vibrations, Magnetic Noise, Maxwell Pressure, Radiated Acoustic Power, Bi-Dimensional FFT, Travelling Waves.

## I. NOMENCLATURE

- $t$  : Time (s)
- $\theta$  : Spatial angle (rad)
- $P_r$  : Radial Maxwell pressure (Pa)
- $B_r$  : Radial flux density (T)
- $\mu_0$  : Vacuum permeability (T.m/A)
- $B_i$  : Magnitude of the travelling wave  $i$
- $\omega_i$  : angular frequency of the travelling wave  $i$
- $k_i$  : Wave number of the travelling wave  $i$
- $\varphi_i$  : Phase-shift of the travelling wave  $i$

## II. INTRODUCTION

NOISE in electric machines can be divided into three categories: magnetic, mechanical and aerodynamic. The magnetic noise, which constitutes the subject of this paper, is mainly due to the radial forces or per unit of area, the radial Maxwell pressure. Indeed, the magnetic flux in the machine passes across the airgap in an approximate radial direction producing radial forces on the stator resulting in vibrations and thus magnetic noise. One of the most efficient ways to cancel and mitigate this kind of noise is to well identify its sources. Thus, it is of importance to know the harmonic content of the radial forces in terms of frequencies and wave numbers. Indeed, if there is coincidence in the spatial and frequency domains between radial forces and the natural behavior of the stator, resonance occurs leading to very high vibrations and acoustic noise. In the case of classical machines, such as induction and synchronous machines, different works have been carried out and a mathematical model of the radial forces has been developed leading to analytical expressions of the frequencies and spatial orders composing the radial

forces [1-6]. These components have different origins, the main ones are stator slot harmonics, rotor slot harmonics, winding harmonics, eccentricities and saturation effect. More specifically, the latter introduces the harmonics shown in Table I [4] which increase the audible noise.

TABLE I  
SPATIAL ORDERS AND FREQUENCIES OF MAIN SATURATION FORCES EXPRESSIONS

	Frequency $f$	Spatial order $m$
$F_{sat}^-$	$f_s(k_r Z_r(1-s)/p - 2(1+k_a))$	$k_r Z_r - k_s Z_s - 2p(1+k_a)$
$F_{sat}^0$	$f_s(k_r Z_r(1-s)/p \pm 2k_a)$	$k_r Z_r - k_s Z_s \pm 2pk_a$
$F_{sat}^+$	$f_s(k_r Z_r(1-s)/p + 2(1+k_a))$	$k_r Z_r - k_s Z_s + 2p(1+k_a)$

In the case of SRMs [7-10], such analytical expressions have not been elaborated. Indeed, as SRMs are not fed through polyphase balanced system simple analytical model of radial forces is quite difficult to develop. Yet, in order to quantify the effect of the different phenomena on the harmonic content of electromagnetic and acoustic fields of SRMs, each effect needs to be isolated and studied. This paper focuses only on the effect of material saturation even if it is inevitably combined with the slotting effect due to the presence of stator and rotor teeth. In order to achieve this, the approach based on the coupling of magnetic, mechanic and acoustic numerical models remains the most accurate way to study such phenomena. But this needs very high calculation times. Another solution consists on using a numerical electromagnetic model based on FEM coupled to analytical mechanic and acoustic models. This approach can give accurate results while saving time calculation [11].

## III. DESCRIPTION OF THE STUDY

### A. Electromagnetic models

To study the saturation effect, an electromagnetic model taking into account the material nonlinearities is needed. Here, Finite Element (FE) models of 4-phase 8/6 and 16/12 SRMs are used. Due to the symmetry, only half and quarter of the motors are modeled respectively for the 8/6 and the 16/12 SRMs as shown in Fig. 1 and Fig. 2. In the time domain, the simulations are performed on one electric period.

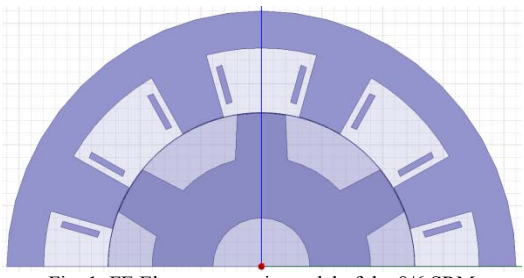


Fig. 1. FE Electromagnetic model of the 8/6 SRM

<sup>1</sup>Laboratoire d'Electrotechnique et d'Electronique de Puissance de Lille, L2EP, Ecole Centrale de Lille, Cité Scientifique, Villeneuve-d'Ascq, France

<sup>2</sup>RENAULT, 1 Avenue du Golf, 78084 Guyancourt CEDEX, France

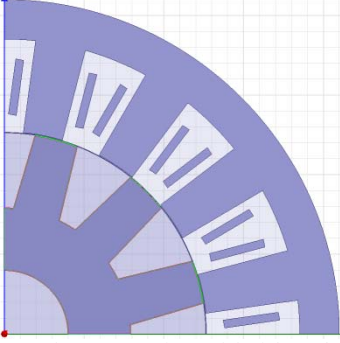


Fig. 2. FE Electromagnetic Model of the 16/12 SRM

### B. Simulations description

Both machines are designed for rated current of 140A. Then, to be sure to investigate the effect of the saturation of the magnetic materials, two simulations are performed for each SRM: 1- Non-saturated case using very low currents magnitudes (10A), 2- Saturated case using a very high currents magnitudes (300A) such that the material will be well saturated. Furthermore, in order to take into account only the nonlinear behavior of the magnetic material, the effect of the control on the phase current is not taken into account. Thus, for both SRMs, the waveforms of the currents supplying the phase winding are theoretical ones as shown below in Fig. 4.

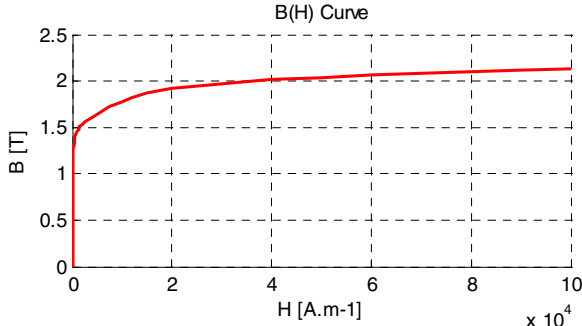


Fig. 3. B-H Curve of the nonlinear material used for 8/6 and 16/12 SRMs

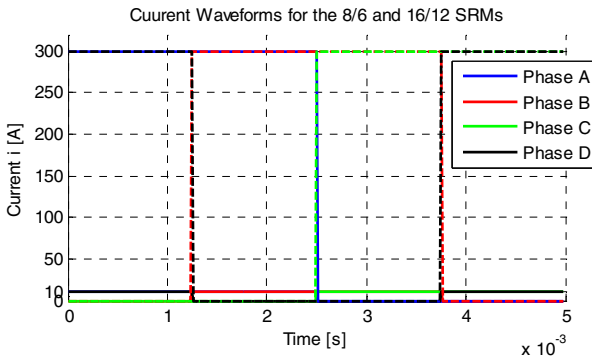


Fig. 4. Current waveforms for the 4-phase 8/6 and 16/12 SRMs

## IV. ANALYSIS OF THE SATURATION EFFECT ON THE ELECTROMAGNETIC RESULTS

### A. Results for the 8/6 SRM

In this work, the effect of the tangential flux density on the acoustic behavior of SRMs is neglected. Thus, in the middle of the airgap, only the radial component of the flux density is studied and analyzed. As a result, the radial Maxwell pressure acting on the stator is approximated by

the following expression:

$$P_r(t, \theta) = \frac{B_r^2}{2\mu_0} \quad (1)$$

In order to analyze the effect of saturation on the harmonic content of the radial flux density and the radial Maxwell pressure, both uni-dimensional (Space or Time) and bi-dimensional (Space and Time) Fast Fourier Transform (FFT) are performed. The radial flux density is then decomposed as a sum of sinusoidal travelling waves:

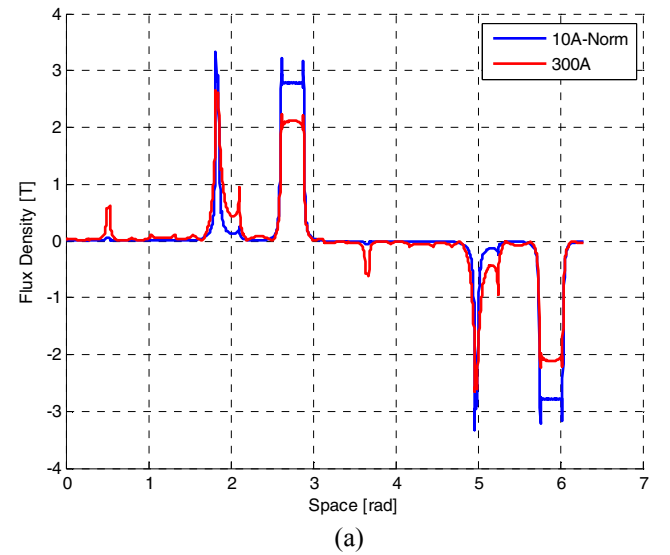
$$B_r(t, \theta) = \sum_i B_i \cos(\omega_i t - k_i \theta + \varphi_i) \quad (2)$$

Using Equation (1), the radial Maxwell pressure can be written as [2]:

$$P_r(t, \theta) = \frac{1}{2\mu_0} \sum_i \frac{B_i^2}{2} [1 + \cos(2\omega_i t - 2k_i \theta + 2\varphi_i)] + \frac{1}{2\mu_0} \sum_i \sum_j B_i B_j [\cos((\omega_i \pm \omega_j)t - (k_i \pm k_j)\theta + (\varphi_i \pm \varphi_j))] \quad (3)$$

Fig. 5 shows the variation of radial flux density, first, as a function of the spatial angle for a given time, and then, as a function of time for a given spatial position. For the 8/6 SRM, even if only half a machine is simulated, the spatial period of the radial flux density is  $[0, 2\pi]$ . Hence, the total radial flux density is built as a periodic odd function being positive on the first half  $[0, \pi]$  and negative on the other half  $[\pi, 2\pi]$  of the spatial period as shown in Fig. 5 (a) and later in Fig. 6.

The difficulty to compare the results between linear and nonlinear electromagnetic fields lies in the fact that the magnitude of the non-saturated radial flux density is significantly higher than the one in the saturated case. In order to bypass this offset, a normalization with respect to the DC component is applied to the non-saturated Maxwell pressure. Hence, the linear and nonlinear magnetic fields have the same mean value. Therefore, all the study is based on this hypothesis, i.e. the following comparisons oppose nonlinear fields to normalized linear ones.



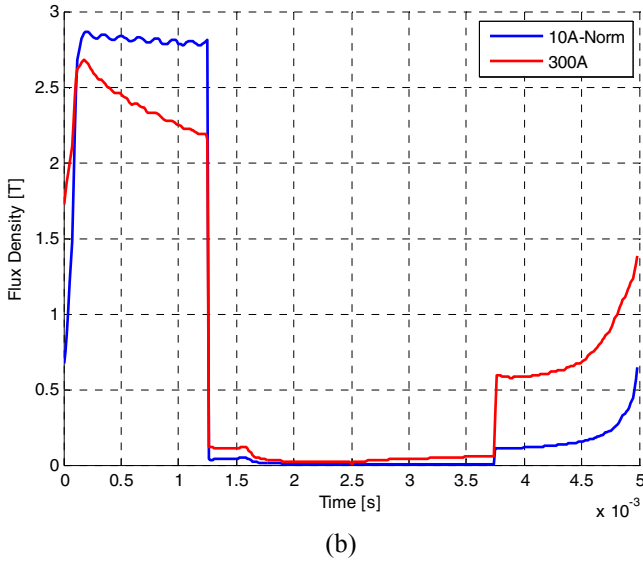


Fig. 5. Radial flux density of the 8/6 SRM ((a) in function of Space for a given time, (b) in function of time for a given position)

In order to illustrate the variation of the flux density on a whole spatio-temporal period, the representation given in Fig.6 is adopted.

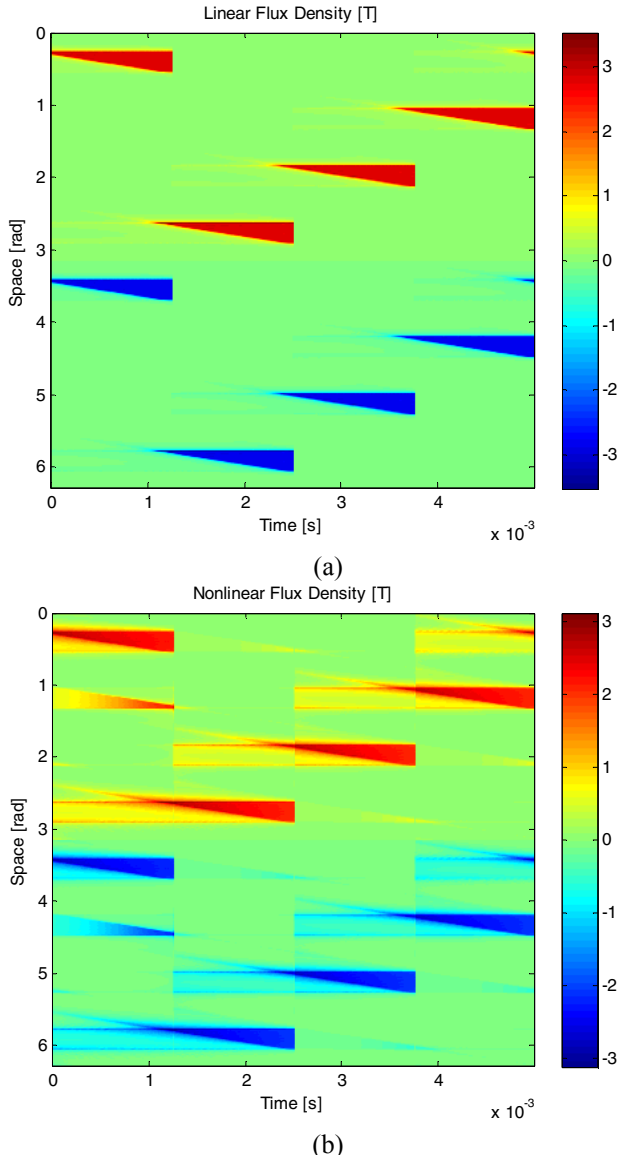


Fig. 6. Radial flux density in function of space and time of the 8/6 SRM ((a) Non-saturated SRM, (b) Saturated SRM)

This representation gives information on the geometric construction of the SRMs. For example the number of stator teeth is given by the number of triangles according to the spatial axis. The number of phases is given by the number of triangles following the time axis. It can also be pointed that in the nonlinear case, the flux density waveform is different. Because of saturation, the flux lines tend to spread out leading to fringing flux which gives this particular waveform of Fig. 6 (b). The bi-dimensional FFT of the radial flux densities are given in Fig.7 using dB scale (Reference 1T).

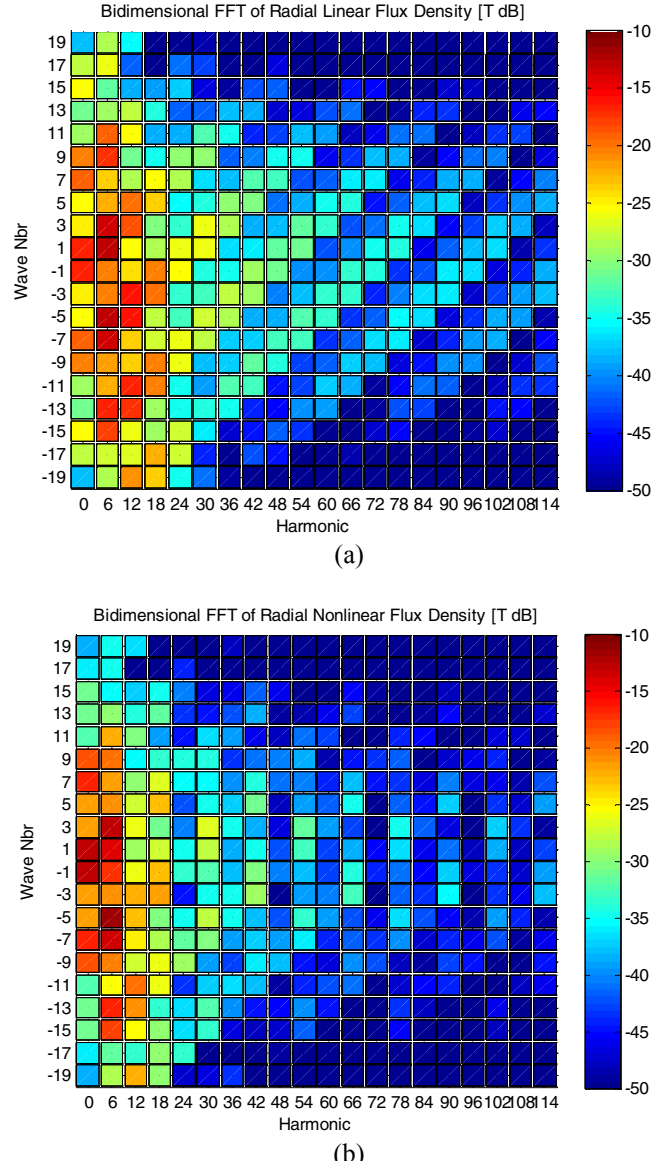
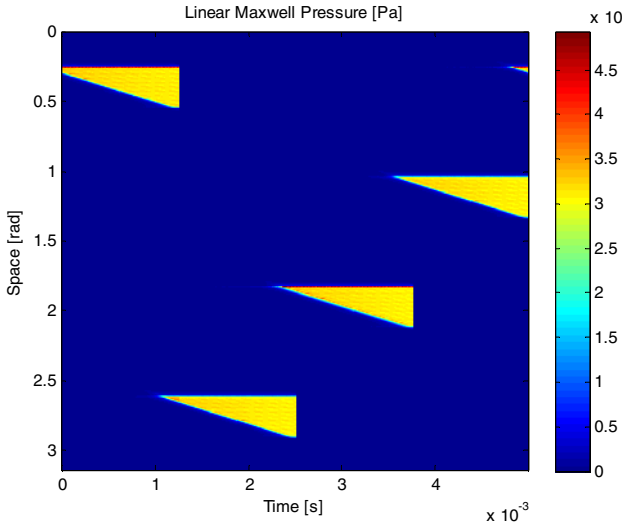


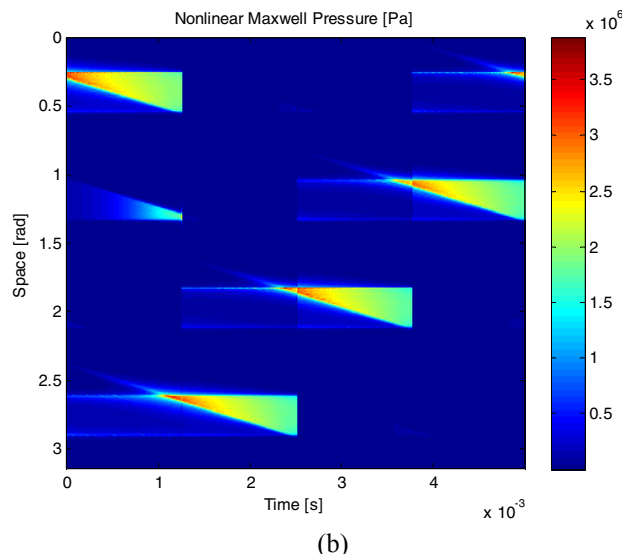
Fig. 7. Radial flux density: Bi-dimensional FFT in function of Harmonic and Wave Number of the 8/6 SRM ((a) Non-saturated SRM, (b) Saturated SRM)

Two observations from Fig. 7 can be highlighted. First, the harmonic step is 6 for the 8/6 SRM. This is consistent with the number of rotor teeth. Second, the wave numbers are odd numbers with a step equal to 1. This is logical because the radial flux density is an odd periodic function according to the space dimension.

Using Equation (1), the variation of the radial Maxwell pressures in function of space and time of the 8/6 SRM is presented in Fig. 8.



(a)

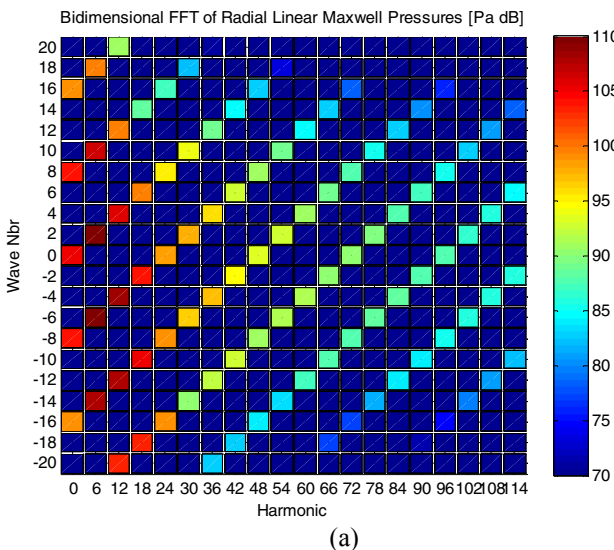


(b)

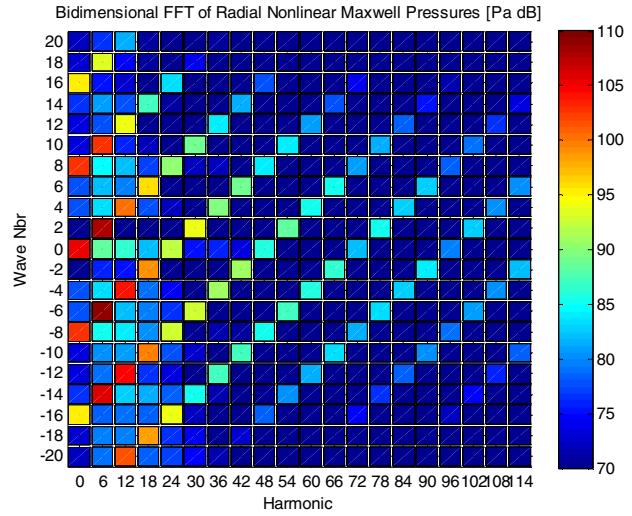
Fig. 8. Radial Maxwell pressure in function of space and time of the 8/6 SRM ((a) Non-saturated SRM, (b) Saturated SRM)

It can be noted from Fig. 8 that, the Maxwell pressure being proportional to the square of the flux density, its spatial period is half the flux density spatial period:  $[0, \pi]$ .

The illustration of the radial Maxwell pressure after bi-dimensional FFT is given in Fig. 9 for the 8/6 SRM in dB scale (Reference 1Pa).



(a)



(b)

Fig. 9. Radial Maxwell pressure Bi-Dimensional FFT of the 8/6 SRM ((a) Non-saturated SRM, (b) Saturated SRM)

A first observation from Fig. 9 concerns the presence of diagonal lines. This is due the slotting effect and will not be analyzed in this paper. Then, the comparison between the harmonic content of saturated and non-saturated radial Maxwell pressure shows that in the case of SRMs, unlike induction motors, there is no additional harmonics due to the saturation effect. However, a difference in the magnitudes mirrored by the difference of colors can be pointed.

So as to quantify more accurately the difference between magnitudes, two separate uni-dimensional FFT on the radial Maxwell pressure are carried out.

In a first step, for a given spatial position, a temporal FFT is performed on the radial Maxwell pressure of the 8/6 SRM leading to results shown in Fig. 10.

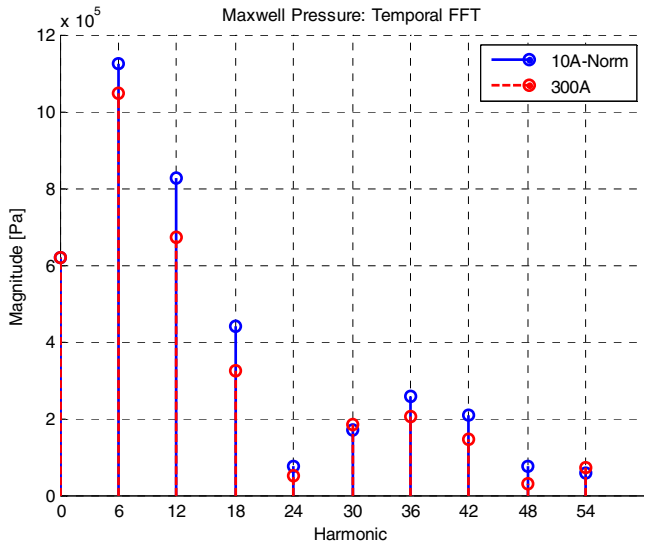


Fig. 10. Temporal FFT on the radial Maxwell pressure at a given position for the 8/6 SRM

Globally, the saturation effect decreases the magnitude of the different temporal harmonics.

Then, for a given time corresponding to the aligned position, a spatial FFT on the radial Maxwell pressure of the 8/6 SRM gives the results presented in Fig. 11.

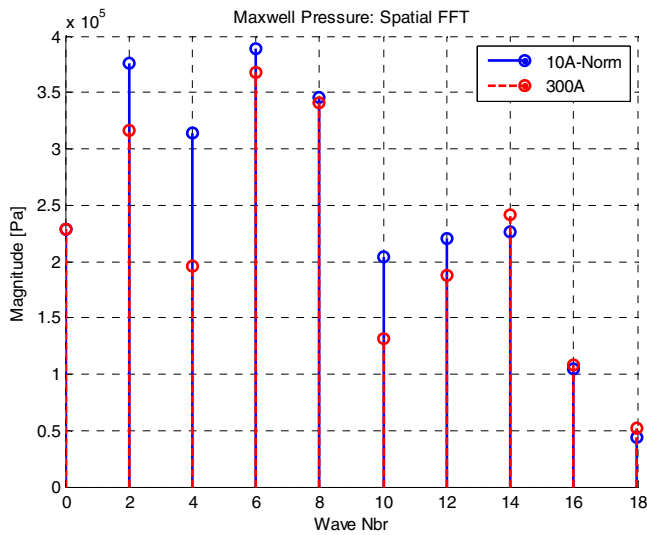


Fig. 11. Spatial FFT on the radial Maxwell pressure at the aligned position for the 8/6 SRM

These results show that the effect of saturation is not uniform on the different spatial harmonics. Nevertheless, low harmonics can be considered as more affected by saturation than higher ones.

In order to have a more general idea of the effect of the saturation according to both spatial and temporal harmonics simultaneously, the difference between the saturated (Fig. 9 (b)) and non-saturated (Fig. 9 (a)) radial Maxwell pressures is achieved. To focus on the main harmonics, only those forming the diagonal lines are kept. The result of this difference is shown in Fig. 12 below.

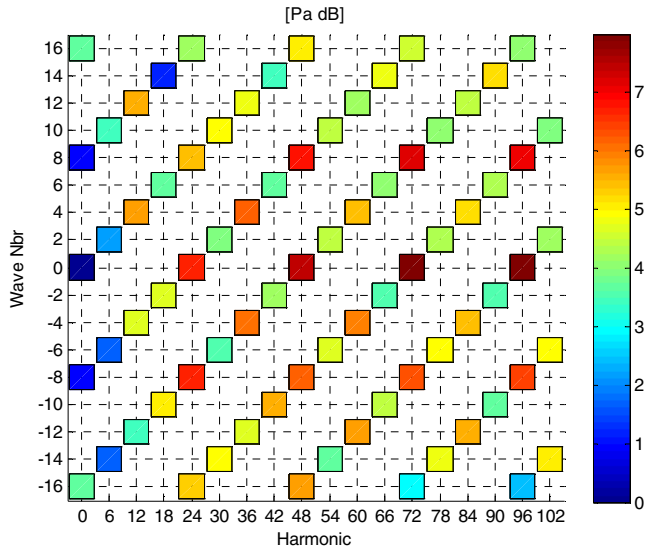


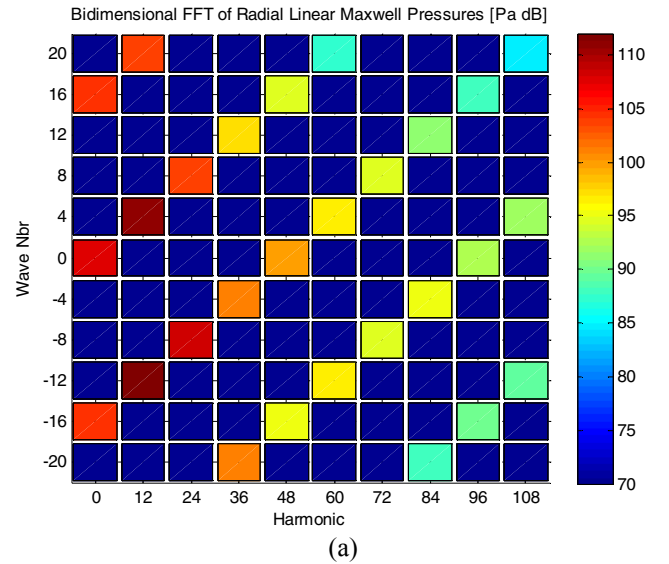
Fig. 12. Difference between the saturated (Fig. 8 (b)) and non-saturated (Fig. 8 (a)) radial Maxwell pressure after bi-dimensional FFT

It can be confirmed from Fig. 12 that the saturation affects non-uniformly the harmonic content of the radial Maxwell pressure. Though, the wave numbers -8, -4, 0, 4 and 8 seem to be the most affected by the saturation in terms of harmonics' magnitude (especially the order 0).

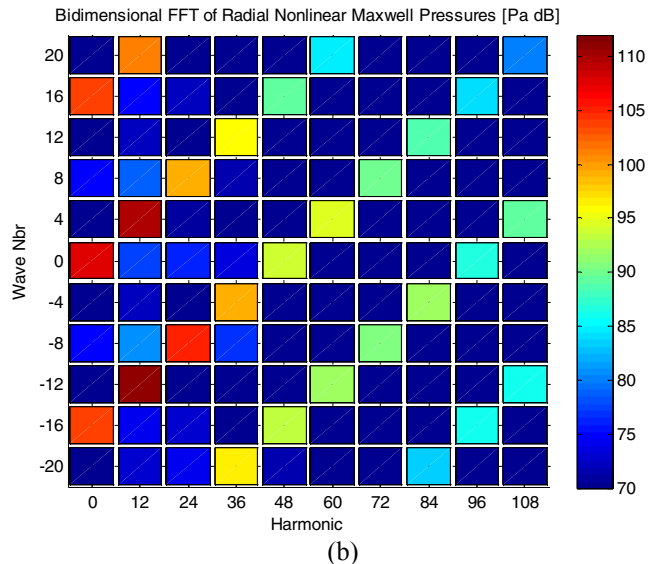
In order to expand this study, the saturation effect is evaluated on a SRM having twice as many teeth as the 8/6 SRM for the same outer diameter. The results on this 16/12 SRM are presented in the following section.

## B. Results for the 16/12 SRM

A bi-dimensional FFT is done on the radial Maxwell pressure of the 16/12 studied SRM as shown in Fig. 13.



(a)



(b)

Fig. 13. Radial Maxwell pressure Bi-Dimensional FFT of the 16/12 SRM ((a) Non-saturated SRM, (b) Saturated SRM)

As expected the spatial and temporal harmonic steps of the 16/12 SRM are different from those of the 8/6 SRM, but they stay relevant with the geometrical data of the 16/12 SRM. Actually, the harmonic step is given by the number of rotor teeth, here 12, and the wave number step is equal to 4 which is meaningful because the spatial period of the 16/12 SRM corresponds to a quarter of the motor as shown in Fig. 2. As for the 8/6 SRM, one can notice the presence of diagonal lines due to the slotting effect and the absence of spectrum enrichment between the saturated and non-saturated cases.

Besides, Fig. 14 and Fig. 15 lead to the same conclusions as for the 8/6 SRM in terms of influence of the saturation on the temporal and spatial harmonics.

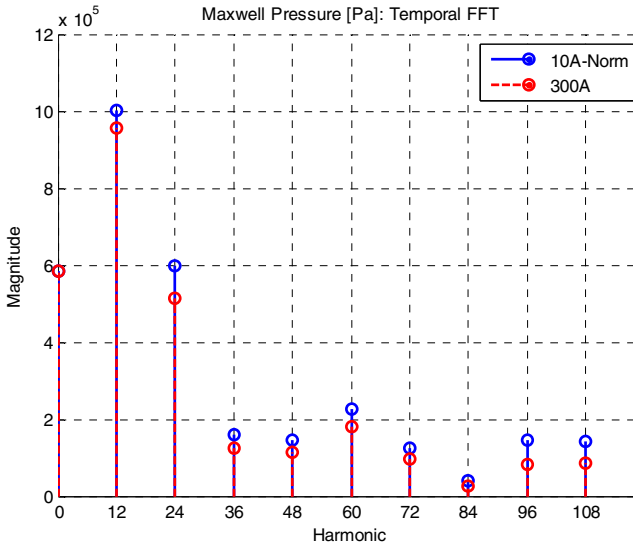


Fig. 14. Temporal FFT on the radial Maxwell pressure at a given position for the 16/12 SRM

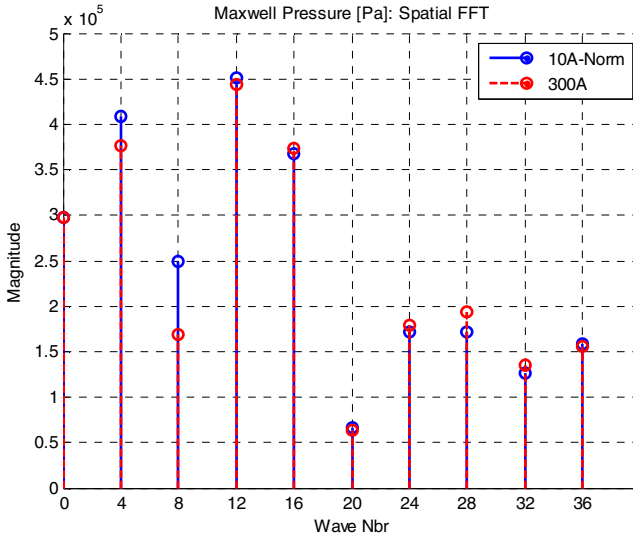


Fig. 15. Spatial FFT on the radial Maxwell pressure at the aligned position for the 16/12 SRM

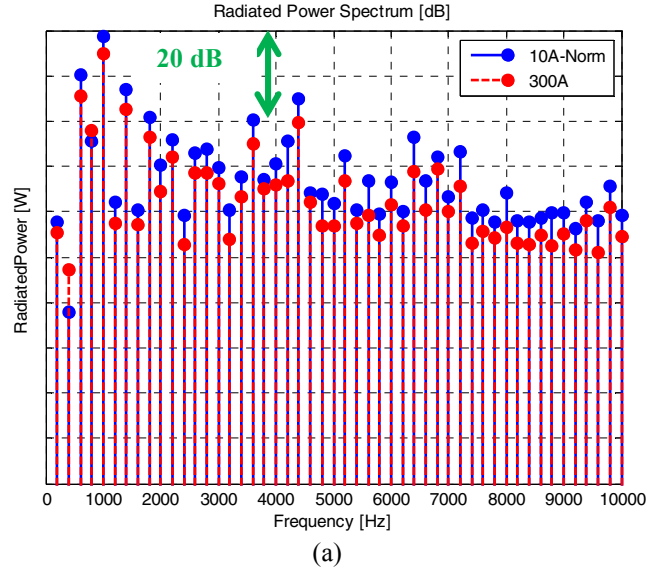
At this stage of the study, it was interesting to describe the influence of the saturation on the electromagnetic fields, but it is difficult to say if this phenomenon will have an influence on the acoustic behavior or not. That is why a vibro-acoustic study was carried out in the following section.

## V. ANALYSIS OF THE SATURATION EFFECT ON THE ACOUSTIC RESULTS

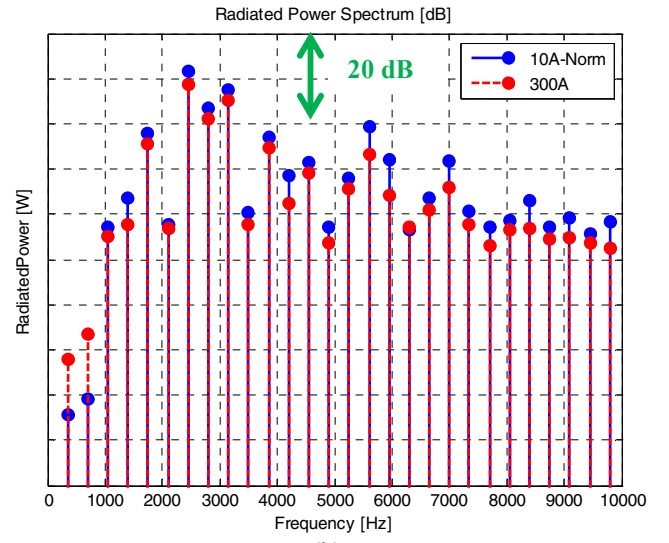
To estimate the radiated acoustic power, vibratory and acoustic models are needed. In this work, the analytical models presented in [12] are used. The vibration model assumes that the deformation of the stator can be approximated by the deformation of a circular beam (Ring) which means that the out-of-plane displacements and shear deformation are neglected. It is also assumed that the straight sections keep their shapes. The acoustic model is based on the Helmholtz equation established in a cylindrical coordinate system. The hypothesis of free-field radiation is made.

To quantify the influence of SRM saturation on their

acoustic behavior, the radial Maxwell pressures presented above with linear and nonlinear simulations are injected in the vibro-acoustic analytical model. The obtained radiated acoustic powers are shown in Fig. 16.



(a)



(b)

Fig. 16. Comparison of radiated acoustic power ((a) 8/6 SRM, (b) 16/12 SRM) between saturated and non-saturated cases

Thanks to the normalization hypothesis mentioned in section IV-A, it is possible to isolate and quantify the saturation effect on the acoustic behavior of SRMs. As a result, one can conclude from Fig. 16 that globally, the saturation effect decreases the magnitude of the radiated power of almost 5dB except for some few low frequencies. So, unlike induction motors where the saturation can sometimes be very annoying, in the case of SRMs, saturation seems to be quite beneficial from an acoustic point of view.

## VI. CONCLUSION

In this paper, the effect of saturation on the electromagnetic and acoustic behavior of two 4-phase SRMs was investigated. It has been shown that, unlike induction motors, the saturation phenomenon does not

induce additional harmonics neither in the space nor in the time domains. The effect of saturation on the motor harmonic behavior was isolated. It appears that the saturation tends to reduce the radiated acoustic power.

## VII. REFERENCES

- [1] J. P. Lecointe, B. Cassoret, and J. F. Brudny, "Distinction of toothings and saturation effects on magnetic noise of induction motors," *Progress In Electromagnetics Research*, vol. 112, pp. 125-137, 2011.
- [2] S. L. Nau, H. G. Gomez Mello, "Acoustic noise in induction motors: Causes and Solutions," *Petroleum and Chemical Industry Conference*, pp. 253-163, 2000.
- [3] P. Vijayraghavan, R. Krishnan, "Noise in electric machines: A review," *IEEE Industry Applications Conference*, vol. 1, pp. 251-258, 1998.
- [4] J. Le Besnerais, V. Lanfranchi, M. Hecquet, and G. Friedrich, "Permeance computation for determination of induction motor acoustic noise," *XIV International Symposium on Electromagnetic Fields in Mechatronics, Electrical and Electronic Engineering*, 2009.
- [5] S. Huang, M. Aydin, T. A. Lipo, « Electromagnetic Vibration and Noise assessment for Surface Mounted PM Machines », *Power Engineering Society Summer Meeting*, Vol. 3, pp 1417-1426, 2001.
- [6] J. F. Gieras, C. Wang, J. C. Lai, "Noise of polyphase electric motors", Taylor and Francis Group, Boca Raton London New York, 2006.
- [7] M. Gabsi, F. Camus, T. Loyau, J. L. Barbry, « Noise reduction of Switched Reluctance Machine », *International Conference Electrical Machines and Drives*, pp 263-265, 1999.
- [8] M. Gabsi, F. Camus, M. Besbes, « Computation and measurement of magnetically induced vibrations of a switched reluctance machine», *IEE Proceedings - Electric Power Applications*, pp 463-470, 1999.
- [9] C. Picod, M. Besbes, F. Camus, M. Gabsi, "Influence of stator geometry upon vibratory behavior and electromagnetic performances of switched reluctance motors", *Eighth International Conference On Electrical Machines and Drives*, pp 69-73, 1997
- [10] J. P. Lecointe, R. Romary, J. F. Brudny, M. McClelland, "Analysis and active reduction of vibration and acoustic noise in the switched reluctance motor", *IEE Proceedings – Electric Power Applications*, Vol. 151, Issue 6, pp 725-733, 2004.
- [11] H. Mechmeche, G. Fritz, F. Gillon, A. Tounzi, and M. Hecquet, "A fast and accurate multi-physic approach to predict acoustic noise:

Applictaion to SRMs", Nineteenth COMPUMAG Conference on the Computation of Electromagnetic Fields, 2013.

- [12] H. Mechmeche, M. Hecquet, F. Gillon, A. Tounzi, and G. Fritz, "Vibration and acoustic noise prediction in an 8/6 SRM using coupled analytical multi-physic models", *XVI International Symposium on Electromagnetic Fields in Mechatronics, Electrical and Electronic Engineering*, 2013

## VIII. BIOGRAPHIES

**Haïfa Mechmeche** (PhD Student) was born in 1988. She graduated from Supméca-Paris (Institut Supérieur de Mécanique de Paris) as an engineer in 2011. She received her Research Master's degree in structural dynamics and coupled systems from Ecole Centrale de Paris (2011).

**Michel Hecquet** was born in 1968. He received the Ph.D degree from the University of Lille, France, in 1995. His Ph.D dissertation presented a 3D permeance network of a claw-pole alternator, used for the simulation and the determination of the electromagnetic forces. Since 2007, he is a professor at Ecole Centrale de Lille in L2EP (Laboratoire d'Electrotechnique et d'Electronique de Puissance). His main interests are the development of multi-physics models of electrical machines (electromagnetic, mechanic and acoustic) and the optimal design of electrical machines.

**Abdelmounaïm Tounzi** (member IEEE), graduated from the University of Nancy - France (M's 1989) and the 'Institut National Polytechnique de Lorraine' (INPL) - France (PhD 1993). From 1993 to 2008, he was an associate professor at the University of Lille 1 (USTL). Currently, he is full professor at the same university. His research areas are the design and modeling of electromagnetic systems.

**Frédéric Gillon** obtained an Engineer Diploma in 1992 and a Ph.D. in 1997 at Université des Sciences et Technologies de Lille. He is currently Assistant Professor at Ecole Centrale de Lille since 1999. These area researches are the Design by Optimization of electric systems and the study of electric machines. The applications are: linear motors, axial and radial synchronous motors, and railway propulsion systems.

**Guillaume Fritz** received a MSc in 2003 and a Ph.D in 2007 in Mechanical Engineering from Ecole Centrale de Lyon. Since 2007, he works at Renault as a NVH research engineer.